Excited States of Porphyrin Isomers and Porphycene Derivatives: A SAC-CI Study

Jun-ya Hasegawa,[†] Koji Takata,[†] Tomoo Miyahara,[†] Saburo Neya,[§] Michael J. Frisch,[∥] and Hiroshi Nakatsuji*,[†,‡]

Department of Synthetic Chemistry and Biological Chemistry, Graduate School of Engineering, Kyoto University, Nishikyo-ku, Kyoto 615-8510, Japan, Fukui Institute for Fundamental Chemistry, Kyoto University, Sakyo-ku, Kyoto 606-8103, Japan, Laboratory of Physical Chemistry, Graduate School of Pharmaceutical Sciences, Chiba University, 1-33, Yayoi-cho, Inage-ku, Chiba 263-8522, Japan, and Gaussian Inc., North Haven, Connecticut 06473-1712

Excited states of free-base porphyrin isomers, porphycene (**Pc**), corrphycene (**Cor**), and hemiporphycene (**hPc**), were studied by the Symmetry-Adapted Cluster (SAC)/SAC-Configuration Interaction (CI) method. The absorption peaks of the porphyrin isomers were assigned on the basis of the SAC-CI spectra. The X, Y, X′, and Y′ bands of the porphyrin isomers, which have weak intensities, are identified. The differences in the Q-band absorptions among the isomers were clearly explained by the four-orbital model. In **Cor** and **hPc**, the wave function of the B-band corresponds to the mixture of the four-orbital excitations and the optically forbidden excitation of free-base porphin (**P**), due to the molecular symmetry lowering in the isomers. The B-band character is described by the five-orbital model in **Pc** and the six-orbital model in **Cor** and **hPc**. Two tetrazaporphycenes and two ring-extended (dibenzo) porphycenes were designed, and the Q-band transition moment was successfully controlled. These examples show that the control of the four-orbital energy levels is the guiding principle for pigment design in porphyrin compounds.

1. Introduction

Tetrapyrrolic macrocycles have intriguing physical, chemical, and biological properties. In biological processes, Fe-porphyrins are found in hemoglobins, myoglobins, and cytochromes, whereas chlorophylls are used in photosynthetic systems. Therefore, tetrapyrrolic molecules are appropriately called the "pigment of life".[1] In the medical field, porphyrins have been used in photodynamic therapy for the treatment of cancer and dermatological diseases.[2,3] In material sciences, phthalocyanines are valuable as components of organic materials and chromophores. These interdisciplinary interests have led to the synthesis of porphyrin isomers. Porphycene was the first isomer to be synthesized.[4] Theoretical studies by Waluk and Michl suggested that other porphyrin isomers also have a porphyrin-like electronic structure.[5,6] This prediction was confirmed by the synthesis of corrphycene[7,8] and hemiporphycene.[9,10] Porphycene has been shown to be a promising compound for photodynamic therapy.[11,12]

There are many theoretical studies on the ground-state structure of the porphyrin isomers. Geometrical isomerism ((E/Z)-configurations)[13] and NH tautomerism of porphycene,[13–16] corrphycene,[7,13] and hemiporphycene[10,13] were theoretically investigated using the density-functional theory (DFT)[13,14,16] and the MP2 method.[15] These studies clarified that the trans isomers with a (Z)-configuration (shown in Figure 1) are more stable than other isomers, although some of the NH tautomers are nearly as stable as the equilibrium structures.[13–16] The relative stability of these four isomers was also investigated by DFT.[17]

However, there are few theoretical studies on the excited states of porphyrin isomers, apart from some semiempirical calculations[5,18] of the excited states of porphycene. Considering the practical applications of porphyrin isomers, a theoretical understanding of the electronic structure of the excited states is very important. Figure 2 shows the experimental absorption spectra of free-base octaethyl-porphin, porphycene, corrphycene, and hemiporphycene.[19] Porphyrin compounds have a weak Q-band around 500–700 nm (1.8–2.5 eV) and a strong B-band around 350–400 nm (3–3.5 eV). Porphycene and hemiporphycene have a much stronger Q-band than porphin and corrphycene. For porphycene, the so-called X- and Y-bands appear in the proximity of the B-band;[5] however, there are no such peaks in the spectrum of porphin.

Here, we briefly introduce Gouterman's four-orbital model[20] and its relation to the absorption spectra of free-base porphin (**P**). Figure 3 shows Hartree–Fock orbital energies of Gouterman's four orbitals (next-HOMO, HOMO, LUMO, and next-LUMO) and several other important orbitals. Arrays and coefficients in the figure show the main configurations and the SAC-CI coefficients of the 1^1B_{3u} (Q_x) and 1^1B_{2u} (Q_y) states of **P**. These two excited states are composed of two near-degenerate excitations within the four-orbitals. This is mainly due to near-degenerate orbital levels. It is also known that the main configuration of the B-band includes an excitation from the fifth orbital (Figure 3).[21ab,22] The intensity of the Q-band is generally weak, since the transition moments of the two near-degenerate configurations cancel each other.[21d] Therefore, a change in the orbital energies relaxes the near-degeneracy, which increases the Q-band intensity. As seen in Figure 3, LUMO and next-LUMO of free-base porphycene (**Pc**) and free-base hemiporphycene (**hPc**) are no longer degenerate, which may result in a more intense Q-band absorption. In addition, the molecular

* To whom correspondence should be addressed. E-mail: hiroshi@sbchem.kyoto-u.ac.jp.
† Graduate School of Engineering, Kyoto University.
‡ Fukui Institute for Fundamental Chemistry, Kyoto University.
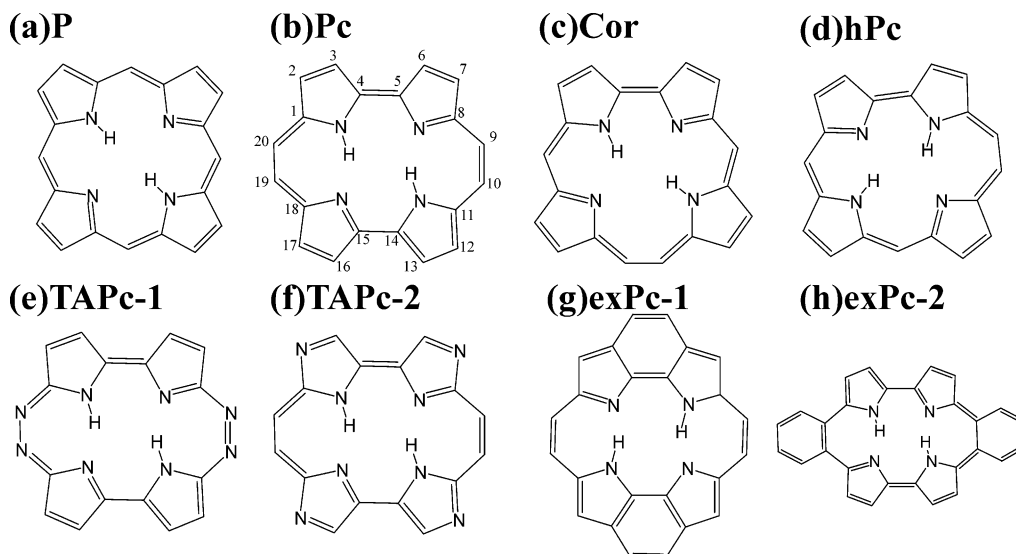§ Chiba University.
∥ Gaussian Inc.

Figure 1. Molecular structure of free-base porphyrin isomers, free-base tetrazaporphycenes, and free-base ring-extended porphycenes. (a) Free-base porphyrin (**P**), (b) free-base porphycene (**Pc**), (c) free-base corrphycene (**Cor**), (d) free-base hemiporphycene (**hPc**), (e) free-base 9,10,19,20-tetrazaporphycene (**TAPc-1**), (f) free-base 2,7,12,17-tetrazaporphycene (**TAPc-2**), (g) free-base 3,6-,13,16-dibenzoporphycene (**exPc-1**), (h) free-base 9,10-,19,20-dibenzoporphycene (**exPc-2**).

structures of **Cor** and **hPc** are reduced to C_s symmetry. This means that the optically forbidden states in **P** and **Pc** can interact with the allowed states. Thus, there are interesting possibilities that structural isomers can direct the molecular design of the excited states. Therefore, quantitative analysis of the excited states by a reliable method is essential.

We have studied the excited states of porphyrin-related compounds,[21] free-base porphin,[21a,b] Mg-porphin,[21c] free-base tetrazaporphin[21d] and phthalocyanine,[21e] hemes,[21f,g,h,j,k] chlorin[21l] and bacteriochlorin,[21l] bacteriochlorophyll-*b*[21i] and bacteriopheophytin-*b*,[21i] and special pair (bacteriochlorophyll-*b* dimer),[21i] using the SAC (Symmetry-Adapted Cluster)[23]/SAC-CI (Configuration Interaction)[24] method.[25] The SAC/SAC-CI method takes into account the electron correlations of the ground and excited states, and its reliability and applicability have been established through a number of applications. This method has precisely reproduced the experimental spectra and clarified the details of the excited states.[25]

The objectives of this study include proposing a reliable theoretical assignment for the absorption spectrum of the porphyrin isomers, analyzing the wave functions of the excited states, and controlling the Q-band transition moment of the porphyrin derivatives by designing the wave function of the excited state. Initially, the excited states of the free-base porphyrin isomers, **Pc**, **Cor**, and **hPc**, were theoretically analyzed using the SAC-CI method. This is the first report that assigns the absorption spectra of porphyrin isomers using a reliable ab initio method. Based on our analysis of the excited states of isomers, we investigated pigment design using the tetraza- (**TAPc-1,2**) and dibenzo-subsitution (**exPc-1,2**) of **Pc**. Similarly substituted porphyrins, tetrazaporphin,[21d,26] and phthalocyanine,[21e,27] showed an increase in their Q-band intensity. The substituted porphycenes studied are shown in Figure 1. To the best of our knowledge, three of these, **TAPc-1**, **TAPc-2**, and **exPc-2**, are newly designed molecules, in which the transition moments of the Q-band were successfully controlled.

2. Computational Details

The molecular geometry of all the molecules in the present study was optimized by DFT[28] (B3LYP[29]). The resultant structures were similar to those reported in a previous article.[13] These studies clarified that the trans-NH tautomers shown in Figure 1 are the most stable. For **exPc-1** (3,6-,13,16-dibenzoporphycene), a planar geometry was assumed. Previously, the absorption spectrum was reported for tetra-*tert*-butyl-3,6-,13,16-dibenzoporphycene[18] which is known to be a planar molecule.[30]

The basis sets for geometry optimizations by DFT and for SAC-CI calculation of the excited states were of valence double-ζ plus polarization quality. In our previous studies,[21] these basis sets provided relatively accurate SAC-CI results for studying the excitation spectrum of porphyrins and related compounds. For **P**, **Pc**, **Cor**, **hPc**, **TAPc-1**, and **TAPc-2**, Huzinaga's (63/5)/[3s2p] sets[31] were used for C and N atoms, and Huzinaga's (4)/[2s] set[32] was used for H atoms. These valence sets were augmented by single polarization functions.[31] Hereafter, we refer to these basis sets as "DZ(d,p)" sets. To optimize the geometry of **exPc-1** and **exPc-2**, 6-31g* sets (6-31G sets[33] plus single polarization d-function[34] on carbon, nitrogen, and oxygen) were used for all the atoms.

For SAC-CI calculations of **P**, **Pc**, **Cor**, **hPc**, **TAPc-1**, and **TAPc-2**, the 57 highest occupied and the 144 lowest unoccupied MOs were included in the active space. This active space was examined by preliminary SAC-CI calculations for **P**. For **exPc-1** and **exPc-2**, the active space consisted of all the valence orbitals. In the SAC/SAC-CI calculations, all the single and selected double excitation operators were included in the wave functions (SAC-CI SD-*R* method). To reduce the computational effort, double excitation operators which gave negligible contributions by a perturbation selection criterion[35] were discarded. Hartree−Fock and single-excitation CI states were used as the reference states of the selections. The double excitation operators which were included had an energy contribution larger than 1×10^{-5} and 1×10^{-6} au for the ground and excited states, respectively. This threshold set is termed as a "Level One" keyword for the SAC-CI method in a suit of new Gaussian programs. The resulting dimensions for the SAC-CI calculations are given in Table 1. As shown in the table, the computational cost can be greatly reduced by the perturbation selection method, which allows for the SAC-CI calculation of relatively large molecules such as the porphyrin compounds.[21]
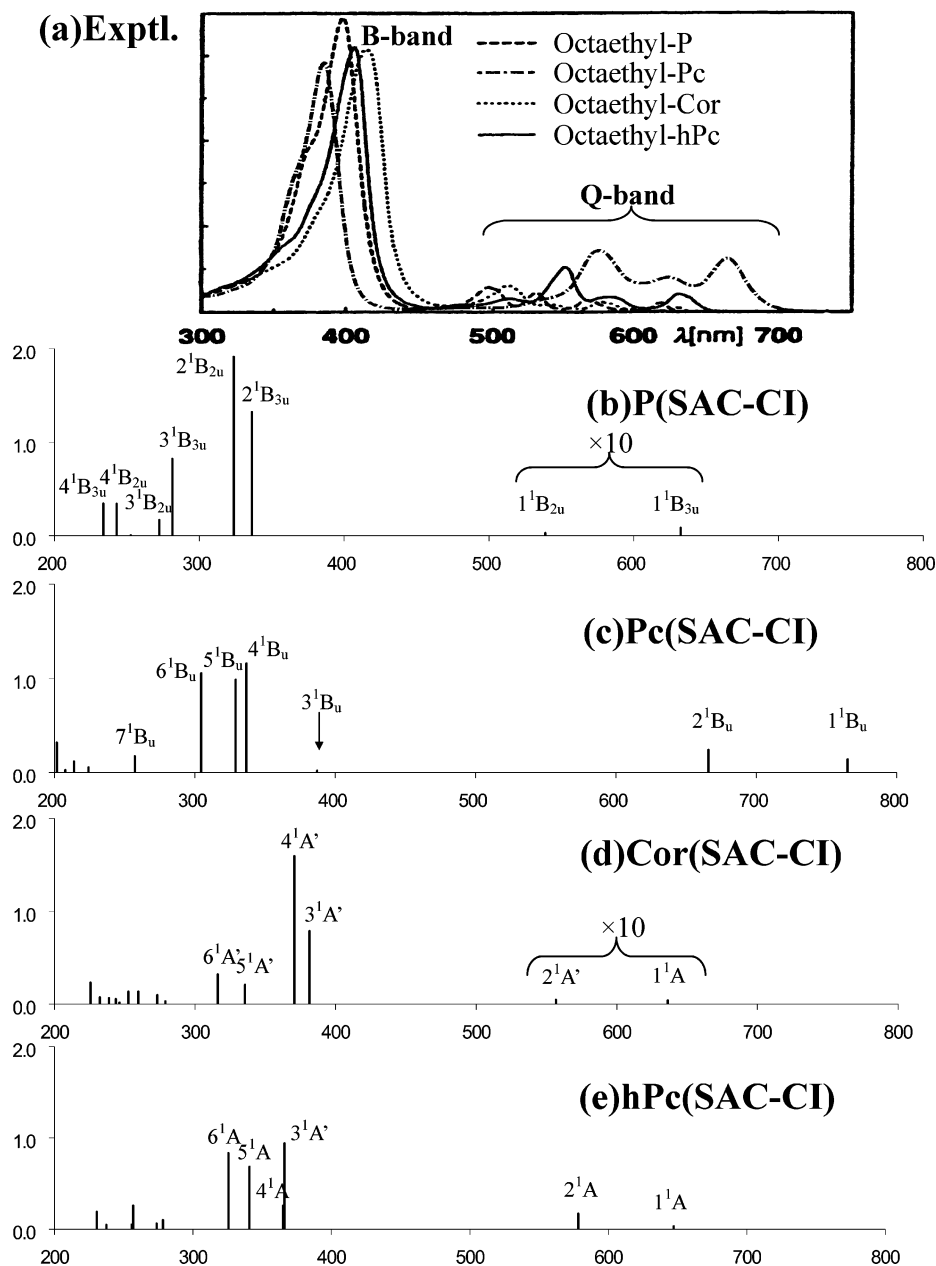
Porphyrin Isomers and Porphycene Derivatives

J. Phys. Chem. A, Vol. 109, No. 14, 2005 **3189**

Figure 2. Excitation spectra of **P**, **Pc**, **Cor**, and **hPc**. (a) Experimental spectra in dichloromethane taken from ref 44 and SAC-CI theoretical spectra for (b) **P**, (c) **Pc**, (d) **Cor**, and (e) **hPc**.

To verify the basis sets effects, additional SAC-CI calculations were performed for **Pc**. The valence basis sets were extended to triple-ζ[36] both for C, N atoms and H atoms. The TZ(2d,p) sets consist of double polarization d functions for the C and N atoms and a single polarization p function for the H atoms.[31] The TZ(d,p)+Ryd. sets include single polarization d and p functions for the C, N atoms and H atoms, respectively. In addition, Rydberg 3s and 3p functions were augmented to the C, N atoms, and 3d functions were augmented to the charge center of the four pyrrole rings. A frozen core approximation was adopted for the SAC-CI calculations, and 612 orbitals were correlated in the largest case. We also improved the thresholds for the perturbation selection to 5×10^{-6} and 5×10^{-7} au (Level Two) for the ground and excited states, respectively.

We also investigated the solvation effect on the excited states of **Pc**. The solvation model used was a PCM model using the integral equation formalism models (IEFPCM),[37] and the dielectric constant of tetrahydrofuran (THF, $\epsilon = 7.58$) was applied to the calculation. The "TZ(d,p)" sets were used as the basis sets.

All calculations were performed using a development version of Gaussian,[38] in which the SAC-CI program had been incorporated. Molecular orbitals were drawn using a MOLDEN visualization software.[39]

3. Results and Discussion

3-1. Ground States of Pc, Cor, and hPc. The energy levels of Hartree−Fock orbitals are shown in Figure 3 for **P**, **Pc**, **Cor**, and **hPc**. The diagram shows Gouterman's four orbitals (next-HOMO, HOMO, LUMO, next-LUMO)[20] and other high-lying occupied orbitals that are important in the excited states. The orbital energy levels of porphyrin isomers have been previously analyzed by perimeter models[5,6] and by the semiempirical INDO method.[18] Therefore, we have highlighted some important
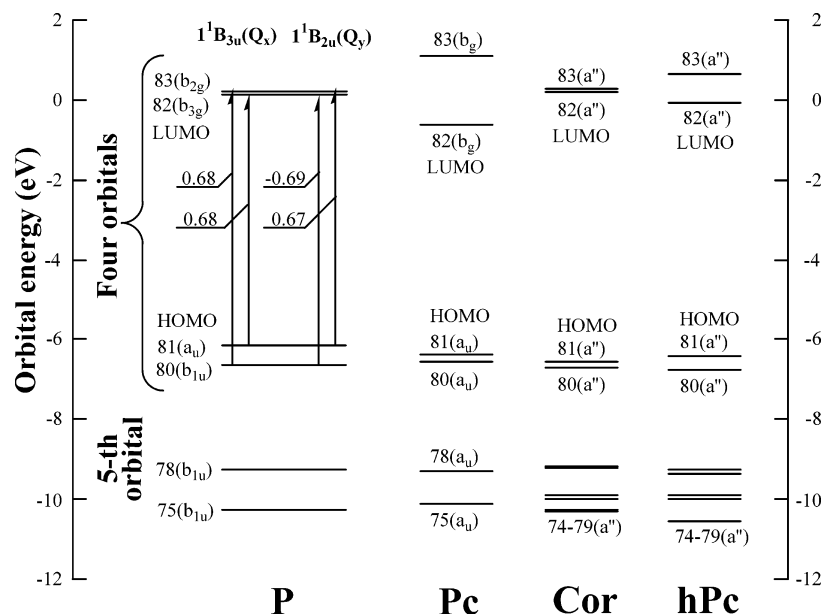
Figure 3. Hartree-Fock orbital energy levels of **P**, **Pc**, **Cor**, and **hPc**. Gouterman's four-orbitals and other orbitals that are important in the excited states are shown. For **P**, the main configurations (indicated by arrays) of the wave function for 1^1B_{3u} (Q_x band) and 1^1B_{2u} (Q_y band) states are also shown. The values shown beside the arrays are coefficients of the main configuration obtained by the SAC-CI calculation.

TABLE 1: Dimensions of the Linked Operator in the SAC/SAC-CI Calculations

	P				**Pc**				**Cor**				**hPc**		
state	N^a	before[b]	after[c]	state	N^a	before[b]	after[c]	state	N^a	before[b]	after[c]	state	N^a	before[b]	after[c]
SAC				SAC				SAC				SAC			
^1A_g	1	4 447 273	25 243	^1A_g	1	8 889 805	18 705	$^1A'$	1	17 836 080	16 137	$^1A'$	1	17 836 080	15 441
SAC-CI				SAC-CI				SAC-CI				SAC-CI			
$^1B_{3u}$	7	4 442 938	94 304	^1A_u	2	7 961 219	60 798	$^1A'$	15	17 836 080	98 240	$^1A'$	12	17 836 080	98 120
$^1B_{2u}$	7	4 442 763	88 831	^1B_u	12	8 885 701	165 067	$^1A''$	15	15 861 864	166 371	$^1A''$	12	15 861 864	125 759
$^1B_{1u}$	1	3 980 928	29 121												

	TAPc-1				**TAPc-2**				**exPc-1**				**exPc-2**		
state	N^a	before[b]	after[c]	state	N^a	before[b]	after[c]	state	n^a	before[b]	after[c]	state	N^a	before[b]	after[c]
SAC				SAC				SAC				SAC			
^1A_g	1	8 778 267	22 511	^1A_g	1	8 804 710	22 236	^1A_g	1	48 983 544	22 343	^1A_g	1	86 889 101	22 049
SAC-CI				SAC-CI				SAC-CI				SAC-CI			
^1A_u	5	8 072 757	127 977	^1A_u	4	8 046 314	94 196	^1B_u	12	48 973 826	190 123	^1B_u	12	86 876 164	179 578
^1B_u	9	8 774 163	112 502	^1B_u	11	8 800 606	163 129								

[a] Number of solution. *[b]* Number of linked operator before selection. *[c]* Number of linked operator after selection.

aspects that are necessary for discussing the excited states. The energy levels were briefly compared in the Introduction.

The energy gap between LUMO and next-LUMO of **Pc** is more remarkable than that of the other isomers. The **hPc** isomer also shows a relatively large energy gap betweeen these MOs. This characteristic is related to the position of the N atoms in the π-conjugation. The degeneracies of the LUMO and the next-LUMO of **P** are perturbed by the displacement of N atoms in **Pc**.[5] Figure 4 shows the molecular orbitals of the four porphyrin isomers. Both LUMO and next-LUMO of **P** have amplitudes on two N atoms, and these orbitals are almost degenerate. On the other hand, LUMO of **Pc** has no amplitude on the N atoms, while next-LUMO has its amplitude on all of the N atoms. A similar situation is seen in **hPc** where LUMO is less populated on the N atoms and next-LUMO is populated on three N atoms. This explanation can also be applied to the energy splitting between the HOMO and next-HOMO levels.

The large energy splitting between LUMO and next-LUMO results in several significant changes in the absorption spectrum of **Pc**: The Q-bands have high intensity, and the X- and Y-bands

appear in the vicinity of the B-bands. In the next subsection, these spectral changes are explained based on the SAC-CI wave functions.

3-2. Excited States of Pc, Cor, and hPc. Figure 2 shows the SAC-CI theoretical spectra of **P**, **Pc**, **Cor**, and **hPc** in a vacuum and the experimental absorption spectra of the octaethyl derivatives in dichloromethane.[19] The SAC-CI spectra reproduced the trends observed in the experimental spectra of the isomers. The average error in the excitation energy is 0.17 eV. The error was relatively large in **Pc** (0.22 eV). Tables 2−6 summarize the SAC-CI results of the dominant configuration, excitation energy, and oscillator strength for the excited states of **P**, **Pc**, **Cor**, and **hPc**.

Excited States of Free-Base Porphin (P). First, we briefly summarize the excited states of **P**, the reference compound among the porphyrin isomers. The dipole-allowed transitions are summarized in Table 2. The detailed assignments and discussions can be found in previous reports.[21a,b,40,41a,b,42a,b] The Q_x- and Q_y-bands are assigned to the 1^1B_{3u} and 1^1B_{2u} states, respectively. The electronic structure of the Q-bands can be described by two degenerate excitations within Gouterman's
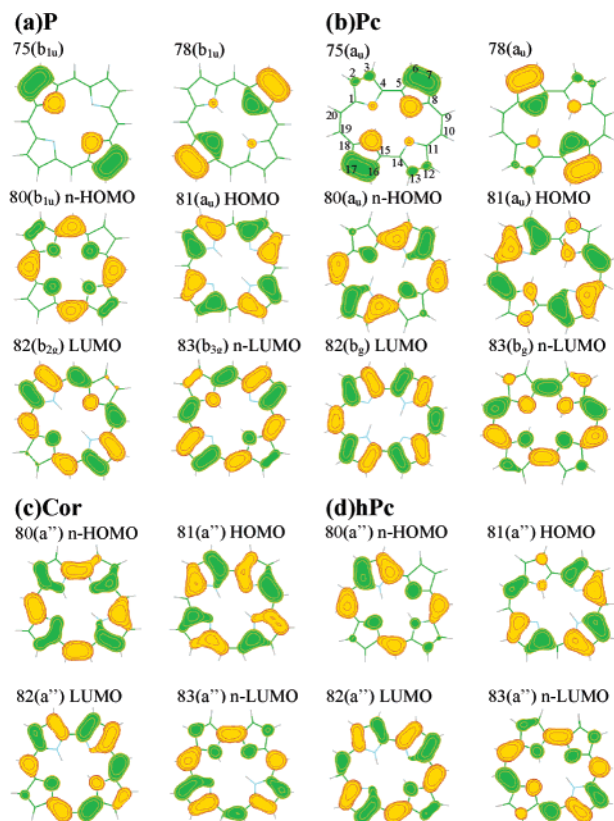
Porphyrin Isomers and Porphycene Derivatives

J. Phys. Chem. A, Vol. 109, No. 14, 2005 **3191**

(a)P
75(b₁ᵤ)   78(b₁ᵤ)
80(b₁ᵤ) n-HOMO   81(aᵤ) HOMO
82(b₂ᵤ) LUMO   83(b₃ₑ) n-LUMO

(b)Pc
75(aᵤ)   78(aᵤ)
80(aᵤ) n-HOMO   81(aᵤ) HOMO
82(bₑ) LUMO   83(bₑ) n-LUMO

(c)Cor
80(a'') n-HOMO   81(a'') HOMO
82(a'') LUMO   83(a'') n-LUMO

(d)hPc
80(a'') n-HOMO   81(a'') HOMO
82(a'') LUMO   83(a'') n-LUMO

Figure 4. Several important molecular orbitals of (a) **P**, (b) **Pc**, (c) **Cor**, and (d) **hPc**.

four orbitals.[20] These two configurations have a similar amount of transition moments but different signs. The oscillator strength of the Q-bands is diminished due to mutual cancellation.[21d] In contrast, these two configurations reciprocally strengthen the transition moments in the B- and N-bands. Therefore, *the oscillator strength of the Q- and B-bands depends on the balance of the weight of the two dominant configurations in the excited states*.

The B- and N-bands are assigned to the 2^1B_{3u} and 2^1B_{2u} states, respectively. *For the B-bands, the four-orbital model is not necessarily valid, since an excitation from orbital 78 ($4b_{3u}$, "fifth MO") to 83 (n-LUMO) becomes one of the main configurations, and thus this should be more appropriately referred to as a "five-orbital model".*[21a,b,22,40b] This excitation 78 → 83 becomes the main configuration of the 3^1B_{3u} state, L-band.

Excited States of Free-Base Porphycene (Pc). Our theoretical assignment for the excitation spectrum of **Pc** is shown in Table 3. Figure 5 compares the SAC-CI theoretical spectrum to the experimental spectrum observed in CH_3CN.[5] The figure also includes the excitation spectra of free-base porphin (**P**) in the gas-phase.[43] SAC-CI calculations reproduced the spectral differences between **P** and **Pc**: the intensity of the Q-bands is much stronger than that of **P**, and the peak position shows a red shift, as seen in Figure 2. The first and second absorption peaks at 1.98 (Q_1-band) and 2.10 eV (Q_2-band) were calculated at 1.62 (1^1B_u state) and 1.86 (2^1B_u state) eV, respectively. The calculation underestimated the excitation energies of the Q-band by about 0.3 eV. The third peak at 2.24 eV was attributed to a vibrational band of the Q_2-band, and there are no electronic states in this region.[5]

The X-band was indicated at the onset of the Soret band, around 3 eV,[5] although this peak was not clearly seen in the experimental spectra shown in Figures 2 and 5. This X-band

was identified in N-protonated porphycene dications.[5] This band is a characteristic feature of the **Pc** spectrum, since **P** does not have an optically allowed excited state in the energy region. Our result confirmed the existence of the X-band. The 3^1B_u state was calculated at 3.20 eV, and the intensity was 10 times smaller than that of the Q-band.

The B- (Soret) bands of **Pc** were observed at 3.35 (B_1) and 3.46 (B_2) eV. These states could be assigned to the 4^1B_u (3.68 eV) and the 5^1B_u state (3.77 eV), respectively. On the higher energy side of the B-band, a broad peak, the Y-band, was observed.[5] The 6^1B_u state calculated at 4.07 eV could be assigned to this peak. The calculated B- and Y-bands reproduced the relative energy among these three states, although the absolute values were uniformly overestimated by about 0.3 eV. Another problem is that the calculated intensity of the 6^1B_u state (1.05) is as large as that of the B-bands. We describe the basis-sets effects later in this subsection. In the energy region higher than 4.5 eV, three peaks were observed at 4.84, 5.23, and 6.19 eV.[5] The 7^1B_u state (4.82 eV) can be assigned to the peak X' at 4.84 eV. The 8^1B_u (5.53 eV) and 9^1B_u (5.80 eV) states are candidates for the peak Y' at 5.23 eV. In this case, the 9^1B_u state would be the tail on the higher energy side of the peak. For the peak at 6.19 eV, we can assign the 11^1B_u state calculated at 6.15 eV. The 10^1B_u state at 5.97 eV would lie on the lower side of the shoulder of the peak. We also calculated the n-π^* transitions as 1^1A_u (4.07 eV) and 2^1A_u (5.53 eV) states. The oscillator strength of these states was too weak to be observed in the experiment.

Next, we discuss the electronic structures of the excited states of **Pc** and compare them with those of **P**. As in the Q-band of **P**, the 1^1B_u (Q_1) and 2^1B_u (Q_2) states are composed of two near-degenerate excitations within the four orbitals. However, the weight of the two configurations of **Pc** is rather different from that of **P**. The ratio of the two main configurations is around 4:1, as shown in Table 3. The leading configurations are 80 (next-HOMO) → 82 (LUMO) and 81 (HOMO) → 82 (next-LUMO) in the 1^1B_u and 2^1B_u states, respectively. As seen in Figure 3, this difference arises from the relatively large energy splitting between LUMO and next-LUMO. *The imbalanced weight of the two main configurations causes an increase in the oscillator strength for the Q-bands*, since the cancellation of the transition moment between the two configurations is incomplete. The relative red shift of the Q-band is also attributed to the stabilization of the LUMO level.

For the 4^1B_u (B_1-band) and 5^1B_u (B_2-band) states, the weight of the two main configurations is also imbalanced as seen in the Q-bands. Consequently, the oscillator strength of the B-bands becomes smaller than that of **P**. This decrease in the oscillator strength is directly related to the increase in the intensity of the Q-band as a result of configuration interactions. Another feature is that excitation from non four-orbitals (75-th MO with a_u symmetry) strongly mixes with the four-orbital excitations. *The four-orbital model is also not valid for the B-band of **Pc**: a five-orbital model would be more suitable for the B-band*. As discussed later with regard to the other compounds, this tendency is generally seen in the porphyrin isomers in this study.

The X-band (3^1B_u state) at 3.10 eV is mainly characterized as the excitation from the 78-th MO (a_u) to LUMO (π-π^* excitation). Based on the similarity in the orbital shape (Figure 4), this excited state corresponds to the 3^1B_{2u} state of **P** (L-band, a broad band on the higher energy side of the B-band). This red shift of the L-band is due to the splitting of the LUMO and next-LUMO levels. On the other hand, excitation from the 78-th MO to next-LUMO (X'-band) shows a blue shift. These

TABLE 2: Excited States of Free-Base Porphin (P) Calculated by the SAC-CI Method

			SAC-CI				exptl		
state	main configurations ($|C| > 0.25$)	nature	excitation energy (eV)	oscillator strength			excitation energy (eV)		
1^1B_{3u}	$0.68(80-83)+0.68(81-82)$	π-π*	1.96	8.4×10^{-3}	x	1.98[a]	2.02[b]	Q_x
1^1B_{2u}	$-0.69(80-82)+0.67(81-83)$	π-π*	2.30	2.8×10^{-3}	y	2.42[a]	2.39[b]	Q_y
2^1B_{3u}	$0.62(81-82)-0.55(80-83)-0.45(78-83)$	π-π*	3.69	1.3	x	3.33[a]	3.17[b]	B
2^1B_{2u}	$0.67(81-83)+0.63(80-82)$	π-π*	3.83	1.9	y	3.65[a]		N
3^1B_{3u}	$-0.81(78-83)+0.37(80-83)-0.25(81-82)$	π-π*	4.41	0.82	x	4.25[a]		L
3^1B_{2u}	$0.88(78-82)+0.33(75-82)$	π-π*	4.55	0.16	y	4.67[a]		L
1^1B_{1u}	$0.95(72-82)$	n-π*	4.91	3.2×10^{-3}	z			
4^1B_{2u}	$0.87(75-82)-0.30(78-82)$	π-π*	5.10	0.34	y			M
4^1B_{3u}	$-0.92(75-83)$	π-π*	5.31	0.34	x	5.50[a]		M
5^1B_{3u}	$-0.89(71-82)$	π-π*	6.82	4.8×10^{-3}	x			
5^1B_{2u}	$0.93(71-83)$	π-π*	6.96	0.2×10^{-3}	y			
6^1B_{2u}	$0.94(80-87)$	π-π*	7.07	0.11	y			
6^1B_{3u}	$0.75(81-87)-0.53(80-86)$	π-π*	7.23	0.03	x			
7^1B_{2u}	$-0.93(81-86)$	π-π*	7.29	3.9×10^{-2}	y			
7^1B_{3u}	$-0.62(80-86)+0.57(79-84)-0.32(81-87)$	π-π*	7.34	1.6×10^{-2}	x			

[a] In vapor phase. Reference 43. [b] In ethanol. Reference 43.

TABLE 3: Excited States of Free-Base Porphycene (Pc) Calculated by the SAC-CI Method

			SAC-CI		CNDO/S[c]	exptl		
						excitation energy (eV)		
state	main configurations ($|C| > 0.25$)	nature	excitation energy (eV)	oscillator strength	excitation energy (eV)	in 2-MTHF[a]	in CH_3CN[a]	in benzene[b]
$1^1B_u(Q_1)$	$0.81(80-82)+0.43(81-83)$	π-π*	1.62	0.141	1.84	1.96(0.12)Q_1	1.98 Q_1	1.97
$2^1B_u(Q_2)$	$0.84(81-82)-0.37(80-83)$	π-π*	1.86	0.241	2.17	2.07(0.16)Q_2	2.10 Q_2	2.08
$3^1B_u(X)$	$0.87(78-82)-0.32(81-83)$	π-π*	3.20	1.75×10^{-2}	3.39	3.10(0.05)X	2.91 X	
$4^1B_u(B_1)$	$0.81(80-83)+0.35(81-82)$	π-π*	3.68	1.16	3.98	3.35(1.32)B_1	3.36 B_1	3.35
$5^1B_u(B_2)$	$0.63(81-83)+0.57(75-82)-0.33(80-82)$	π-π*	3.77	0.984	4.33	3.47(1.32)B_2	3.48 B_2	3.46
1^1A_u	$0.94(72-82)$	n-π*	4.07	0.00				
$6^1B_u(Y)$	$-0.73(75-82)+0.39(81-83)-0.30(80-82)$	π-π*	4.07	1.05	4.95	3.72 Y		
$7^1B_u(X')$	$0.91(78-83)$	π-π*	4.82	0.173		4.84		
2^1A_u	$0.94(72-83)$	n-π*	5.53	3.90×10^{-3}				
$8^1B_u(Y')$	$-0.87(75-83)+0.32(80-86)$	π-π*	5.53	5.41×10^{-2}		} 5.23		
9^1B_u	$0.73(71-82)+0.57(81-86)$	π-π*	5.80	0.117				
10^1B_u	$0.74(81-86)-0.57(71-82)$	π-π*	5.97	2.55×10^{-2}				
11^1B_u	$0.87(80-86)+0.32(75-83)$	π-π*	6.15	0.317		6.19		
12^1B_u	$-0.81(79-84)-0.29(79-85)$	π-π*	7.28	0.273				

[a] Value in parentheses is oscillator strength. Reference 5. [b] Free-base octaethylporphycene. Reference 4. [c] Reference 5.

TABLE 4: Basis Sets Dependency on the Excited States of Free-Base Porphycene Calculated by the SAC-CI Method

	DZ(d,p)		TZ(2d,p)		TZ(d,p)+Ryd.		TZ(d,p) with PCM		ZINDO		exptl	
state	E_{ex}[a]	Osc.	E_{ex}[a]	Osc.	E_{ex}[a]	Osc.	E_{ex}[a]	Osc.	E_{ex}[a]	Osc.	E_{ex}[a]	
1^1B_u	1.62	0.141	1.41	0.1174	1.44	0.1209	1.41	0.1103	1.69	0.0814	1.96[b], 1.98[c]	Q_1
2^1B_u	1.86	0.241	1.63	0.1838	1.68	0.1949	1.63	0.1783	1.83	0.2221	2.07[b], 2.10[c]	Q_2
3^1B_u	3.20	0.018	2.84	0.0035	2.94	0.0044	2.98	0.0156	not obtained		3.10[b], 2.91[c]	X
4^1B_u	3.68	1.160	3.41	0.9174	3.51	0.9749	3.43	1.0089	3.33	1.5858	3.35[b], 3.36[c]	B_1
5^1B_u	3.77	0.984	3.51	0.6032	3.59	0.7315	3.51	0.6942	3.18	1.3516	3.47[b], 3.48[c]	B_2
6^1B_u	4.07	1.050	3.76	1.3437	3.85	1.2782	3.78	1.1911	3.66	1.2768	3.72[b]	Y

[a] Excitation energy in eV unit. [b] In 2-MTHF. [c] In CH_3CN.

corresponding features are indicated by the dotted line in Figure 5. The same feature can be seen for the Y-band, which is characterized as an excitation from the 75-th MO (a_u) to LUMO. This excitation corresponds to the 4^1B_{3u} state (M-band) of **P**. The counterpart of the Y-band is the Y′-band (8^1B_u state), which shows a blue shift from the M-band position in the spectrum of **P**.

Briefly, *stabilization of the LUMO level (large energy-splitting between LUMO and next-LUMO levels) is responsible for most of the spectral features in the spectrum of **Pc***.

The present SAC-CI result of **Pc** shows a relatively large disagreement with the experimental peak positions: an underestimation of 0.34 eV in the 1^1B_u state and an overestimation of 0.33 and 0.30 eV in the 4^1B_u and 5^1B_u states, respectively. We investigated the basis sets effects and the solvation effects.

The results are shown in Table 4. First, the basis sets were extended from DZ(d,p) to TZ(2d,p) sets. The calculated excitation energy uniformly decreases by approximately 0.2−0.3 eV. Although the disagreements in the Q-bands worsened, the excitation energies of the B_1, B_2, and Y bands closely agreed with the experimental values. Inclusion of the Rydberg functions (TZ(d,p)+Ryd.) yielded results which were very close to the TZ(2d,p) result. Therefore, the improvement in the valence basis sets caused a uniform red shift, and the Rydberg functions have little effect on the excitation energy of the six states. The improvement in the basis sets does not improve the intensity of the SAC-CI spectrum. In other words, the DZ(d,p) results are still useful for assigning the experimental spectrum.

The solvation effect also provided only minor corrections, as seen in Table 4. Compared with the TZ(2d,p) results, only

Porphyrin Isomers and Porphycene Derivatives

J. Phys. Chem. A, Vol. 109, No. 14, 2005 **3193**

TABLE 5: Excited States of Free-Base Corrphycene (Cor) Calculated by the SAC-CI Method

| | SAC-CI | | | | exptl[a] |
| | | | excitation | oscillator | excitation |
state	main configurations (|C| > 0.25)	nature	energy (eV)	strength	energy (eV)
1¹A′ (Q₁)	−0.56(81−83)+0.55(80−82)−0.38(81−82)−0.34(80−83)	π-π*	1.95	4.0×10^{-3}	1.96
2¹A′ (Q₂)	−0.59(81−82)−0.54(80−83)+0.38(81−83)−0.36(80−82)	π-π*	2.23	4.6×10^{-3}	2.30
3¹A′ (B₁)	0.60(80−82)+0.56(81−83)−0.32(79−83)−0.26(78−82)	π-π*	3.25	0.787	2.98
4¹A′ (B₂)	0.68(80−83)−0.62(81−82)	π-π*	3.35	1.595	
5¹A′	0.80(79−83)+0.33(79−82)+0.27(81−83)	π-π*	3.69	0.209	
6¹A′	0.76(78−82)−0.41(78−83)+0.26(80−82)	π-π*	3.92	0.319	
1¹A″	0.75(73−83)+0.54(73−82)	n-π*	4.13	7.0×10^{-4}	
2¹A″	−0.72(72−82)+0.55(72−83)	n-π*	4.22	6.0×10^{-4}	
7¹A′	0.62(79−82)+0.49(78−83)+0.27(77−82)	π-π*	4.45	0.0290	
8¹A′	−0.56(79−82)+0.50(78−83)+0.30(77−83)+0.29(78−82)	π-π*	4.54	0.0965	
9¹A′	−0.62(76−82)+0.38(76−83)−0.33(75−83)+0.29(75−82)	π-π*	4.77	0.134	
10¹A′	−0.55(77−82)−0.53(77−83)+0.40(78−83)+0.25(78−82)	π-π*	4.91	0.136	
11¹A′	−0.52(77−82)+0.49(77−83)−0.38(76−82)−0.27(80−84) +0.27(75−83)	π-π*	5.03	0.0169	
3¹A″	0.73(73−82)−0.51(73−83)	n-π*	5.04	7.0×10^{-4}	
12¹A′	−0.57(75−83)+0.40(81−84)−0.30(77−82)+0.27(77−83) +0.26(76−83)	π-π*	5.09	0.0544	
4¹A″	−0.71(72−83)−0.55(72−82)	n-π*	5.13	8.0×10^{-4}	
13¹A′	0.61(80−84)+0.52(75−82)	π-π*	5.19	0.0656	

[a] Etiocorrphycene in benzene. Reference 7.

TABLE 6: Excited States of Free-Base Hemiporphycene (hPc) Calculated by the SAC-CI Method

| | SAC-CI | | | | exptl[a] |
| | | | excitation | oscillator | excitation |
state	main configurations (|C| > 0.25)	nature	energy (eV)	strength	energy (eV)
1¹A′ (Q₁)	−0.78(80−82)+0.51(81−83)	π-π*	1.92	0.0308	1.96
2¹A′ (Q₂)	−0.84(81−82)−0.44(80−83)	π-π*	2.14	0.1688	2.25
3¹A′ (B₁)	−0.71(81−83)−0.46(78−82)−0.37(80−82)	π-π*	3.39	0.9404	3.06
4¹A′	−0.67(79−82)−0.50(80−83)−0.25(78−82)	π-π*	3.40	0.2566	
5¹A′ (B₂)	−0.61(79−82)+0.55(80−83)−0.32(81−82)	π-π*	3.64	0.6826	
6¹A′ (X)	−0.67(78−82)+0.37(80−83)+0.31(80−82)+0.28(81−83)	π-π*	3.81	0.8328	
1¹A″	0.71(72−82)−0.50(73−82)+0.34(72−83)	n-π*	4.12	2.0×10^{-4}	
2¹A″	−0.71(73−82)−0.49(72−82)+0.35(73−83)	n-π*	4.18	3.0×10^{-4}	
7¹A′ (Y)	0.84(75−82)+0.35(76−82)	π-π*	4.46	0.0990	
8¹A′	0.69(76−82)+0.50(77−82)−0.27(75−82)	π-π*	4.53	0.0597	
9¹A′	−0.59(77−82)−0.42(81−84)+0.26(76−82)+0.26(78−83) +0.25(79−83)	π-π*	4.83	0.2585	
10¹A′ (X′)	0.80(78−83)−0.28(79−83)	π-π*	4.85	0.0504	
11¹A′	−0.68(81−84)−0.35(80−84)+0.32(77−82)−0.26(74−82) −0.26(79−83)	π-π*	5.22	0.0456	
3¹A″	−0.82(73−83)−0.26(73−82)	n-π*	5.24	9.0×10^{-4}	
4¹A″	0.82(72−83)−0.28(72−82)	n-π*	5.34	1.7×10^{-4}	
12¹A′ (Y′)	0.65(75−83)−0.39(80−84)+0.31(81−84)−0.30(74−82)	π-π*	5.38	0.1903	

[a] Octaethyl-hemiporphycene. Reference 10.

3^1B_u state shows a small blue shift by 0.15 eV. This could be ascribed to the CT character of the 3^1B_u state. As seen in Figure 4, the 78-th orbital is localized on the two pyrrole rings, while LUMO is delocalized over the molecule.

Finally, the results obtained from other methods are discussed. Previous CNDO/S results, shown in Table 3, reproduced the position of the Q-bands.[5] However, there were significant disagreements in the results of the X, B₁, B₂, and Y bands. The ZINDO results are also shown in Table 4, and the excitation energy values obtained are close to those obtained experimentally. However, we could not obtain the X-band, even though the number of solutions was increased. The order of the B₁ and B₂ bands are different from those obtained by the SAC-CI results. The spectral intensity obtained by ZINDO was similar to that obtained by SAC-CI.

Excited States of Free-Base Corrphycene (Cor). Table 5 shows the SAC-CI results for the excited states of **Cor**. This table also includes the experimental peak positions of etiocor-rphycene in benzene.[7] The first and second peaks observed at 1.96 and 2.30 eV (Q-band) are assigned to the 1¹A′ (1.95 eV)

and 2¹A′ (2.23 eV) states, respectively. As seen in Table 5, the wave functions of these states are composed of all the four excited configurations within the four orbitals. This looks very complicated at first glance but can be easily understood as the mixing of the two excited states (Q_x- and Q_y-bands) of **P**. We can identify two pairs of main configurations, Θ_1 and Θ_2, where Θ_1 is a linear combination of two configurations, 81 (HOMO) → 83 (next-LUMO) and 80 (next-HOMO) → 82 (LUMO), while Θ_2 is a linear combination of 81 → 82 and 80 → 83. The Θ_1 and Θ_2 configurations correspond to the main configurations of the Q_x- and Q_y-bands of **P**, respectively. The Θ_1 and Θ_2 configurations mix with different signs in the 1¹A′ and 2¹A′ states. This state mixing originates from symmetry lowering in the molecular structures from D_{2h} (**P**) to C_s (**Cor**). The oscillator strength of the 1¹A′ and 2¹A′ states is very weak, since these states originate from the Q-bands of **P**.

The main peak of the B-band (2.98 eV) is assigned to the composite of the 3¹A′ and 4¹A′ states, calculated at 3.25 and 3.35 eV, respectively. The main configurations of the 3¹A′ state are two four-orbital excitations and other excitations from non
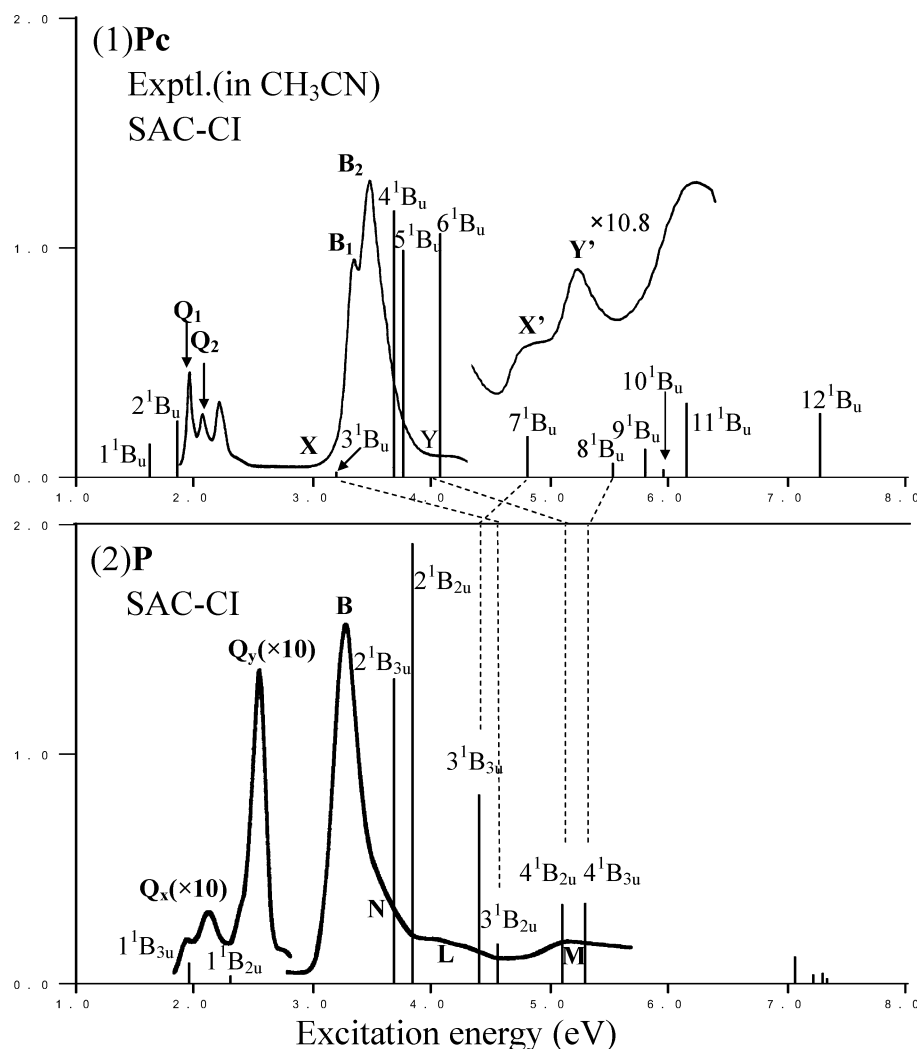
Figure 5. Electronic excitation spectra of (1) **Pc** (experimental spectrum in CH$_3$CN[5] and theoretical spectrum by the SAC-CI method) and (2) **P** (experimental spectrum in vapor phase[43] and theoretical spectrum by the SAC-CI method). The dotted lines show the corresponding states between **P** and **Pc**. The experimental spectra with relative intensity are shown.

four-orbitals: 78- and 79-th MOs. We can observe another effect of symmetry lowering in the molecular structure. The excitation from the 79-th MO to 83-rd MO (LUMO) is similar to the excitation 79 → 83 in **P**. Since the configuration 79 → 83 (next-LUMO) of **P** has gerade symmetry, this transition is optically forbidden. *The B-band (3^{1}A$'$ state) of **Cor** can be characterized as the composite of the 2^{1}B$_{3u}$ (B-band) and the optically forbidden 1^{1}B$_{1g}$ states of **P*** (see ref 21 (a)). Therefore, the oscillator strength of the 3^{1}A$'$ state is smaller than that of the 2^{1}B$_{3u}$ state of **P**, as seen in Table 5. The 78-th MO is characterized as the "fifth MO", since it has a shape similar to the 78-th MO (4b$_{1u}$) of **P**. Therefore, the *B-band of **Cor** should be more appropriately termed as the "six-orbital" model*. On the other hand, the 4^{1}A$'$ state is characterized as a pure four-orbital excited state, and the intensity is much greater than that of the 3^{1}A$'$ state. The excitation energies of the 3^{1}A$'$ and 4^{1}A$'$ states are calculated to be lower than those of **P**, which agrees with the experimental observation.

A shoulder observed in the range 3.5−4.0 eV is assigned to the 5^{1}A$'$ (3.69 eV) and 6^{1}A$'$ (3.92 eV) states. The main configuration of the 5^{1}A$'$ state is the excitation 79 → 83 (next-LUMO), which corresponds to the optically forbidden 1^{1}B$_{1g}$ state of **P**. Since symmetry lowering allows this state to mix with the four-orbital excitations, the 5^{1}A$'$ state gains in intensity. The main configuration of the 6^{1}A$'$ state is the excitation 78 →

82 (LUMO). This state corresponds to the L-band of **P** and to the X-band in **Pc**.

In the higher energy region, above the 6^{1}A$'$ state up to 5.2 eV, our calculation predicted 11 excited states. The spectral features in this region are more complex than those of **P** and **Pc**, since the optically forbidden states in **P** and **Pc** are optically allowed in **Cor**. The n-π* transitions, 1^{1}A$''$ and 2^{1}A$''$ states, were calculated at 4.13 and 4.22 eV, respectively. Two pairs of excited states, 7^{1}A$'$ (4.45 eV) and 8^{1}A$'$ (4.54 eV) states, are characterized as a mixture of the 3^{1}B$_{3u}$ (L-band) and 2^{1}A$_g$ (4.25 eV; optically forbidden) states of **P**. An excited state that corresponds to the M-band of **P** was calculated at 4.77 eV (9^{1}A$'$). The 10^{1}A$'$ (4.91 eV) and 11^{1}A$'$ (5.03 eV) states are related to the 4^{1}A$_g$ state of **P**, which is also optically forbidden.

Excited States of Free-Base Hemiporphycene (hPc). Table 6 summarizes the excited states of **hPc**, and the excitation energies are compared with the experimental spectrum of free-base octaethyl-hemiporphycene.[10] The first peak observed at 1.96 eV is assigned to the 1^{1}A$'$ state calculated to be 1.92 eV. This state is represented by two near-degenerate configurations within the four-orbitals: excitations 80-th MO (next-HOMO) → 82-nd MO (LUMO) and 81-st MO (HOMO) → 83-rd MO (next-LUMO). The ratio of the weight of these two configurations is around 2:1. Thus, this ratio lies between that of the 1^{1}B$_{3u}$ state of **P** (1:1) and that of the 1^{1}B$_u$ state of **Pc** (4:1).

Porphyrin Isomers and Porphycene Derivatives

J. Phys. Chem. A, Vol. 109, No. 14, 2005 **3195**

Therefore, the spectral intensity (0.0308) of the Q$_1$-band also lies between that of **P** (8.4 × 10^{-3}) and **Pc** (0.141), which agrees with the experimental observation[19] shown in Figure 2. This spectral property is related to the energy-splitting of the LUMO and next-LUMO levels, as seen in Figure 3. The 2^{1}A′ state calculated at 2.14 eV is attributed to the second peak observed at 2.25 eV. The main configurations of this state are also two near-degenerate configurations within the four-orbitals, and their weight is imbalanced as in the 1^{1}A′ state.

Regarding the absorption in the 300−450 nm region, the present calculation indicated four excited states that have complex electronic structures. There are two reasons for this complication. First, the LUMO level of **hPc** is relatively low, as in **Pc**, which stabilizes excitation to LUMO. Second, since the molecular symmetry of **hPc** is lower than that of **P** and **Pc**, optically forbidden transitions in **P** and **Pc** can interact with allowed transitions, as explained in the excited states of **Cor**. The 3^{1}A′ (3.39 eV) state accounts for the main peak of the B-band, and the less intense 4^{1}A′ (3.40 eV) state might be hidden by the strong absorption. The main configuration of the 3^{1}A′ state is excitation within the "five-orbitals". For the 4^{1}A′ state, the leading configuration is 79 → 82 (LUMO). Although this configuration is qualitatively equivalent to the optically forbidden configuration of **P** and **Pc**, symmetry lowering allows the interaction with four-orbital excitations.

The broad and strong shoulder on the blue side of the B-band might be assigned to the 5^{1}A′ (3.64 eV) and 6^{1}A′ (3.81 eV) states. The character of the 5^{1}A′ state is a mixture of the excitation 79 → 82 and the ordinary four-orbital excitations of the B-band. These 4^{1}A′ and 5^{1}A′ states have a relatively weak oscillator strength, since the dominant configurations correspond to the forbidden states of **P**. The 6^{1}A′ state corresponds to the L-band of **P** and X-band of **Pc**. Due to the energy level of LUMO, the excitation energy of the 6^{1}A′ state lies between that of the L-band (**P**) and X-band (**Pc**).

The present results show 10 states in the energy region of 4.0−5.5 eV. The 7^{1}A′ state corresponds to the M-band of **P** and the Y-band of **Pc**. Due to the stabilization of the LUMO level, the excited state is shifted by ∼0.6 eV compared to the 4^{1}B$_{2u}$ state of **P**. The counterparts of the 6^{1}A′ and 7^{1}A′ states that correspond to the X′- and Y′-bands of **Pc**, respectively, are the 10^{1}A′ and 12^{1}A′ states calculated at 4.85 and 5.38 eV. For the n-π* transition, the present calculation gave 1−4^{1}A″ states calculated at 4.12, 4.18, 5.24, and 5.34 eV. Their intensity should be very low according to the SAC-CI result. The 8^{1}A′, 9^{1}A′ and 11^{1}A′ states correspond to the optically forbidden states of **P**.

The Transition Moment of the Q-Band of the Four Isomers. We summarize the transition moment of the Q-band of the four isomers. The relative intensity of the Q-band of **Pc** and **hPc** is stronger than that of **P** and **Cor**. In the case of **P** and **Cor**, the Q-bands are composed of the near-degenerate excitations within the four orbitals, since the energy gaps between the LUMO and next-LUMO and between the HOMO and next-HOMO are very small. However, the weight of the two configurations changes to approximately 4:1 in **Pc** and approximately 2:1 in **hPc**, since the energy difference between LUMO and next-LUMO of **Pc** and **hPc** is much larger than that of **P** and **Cor**. The imbalanced weight of the two configurations causes an increase in the oscillator strength of the Q-band, due to the incomplete cancellation of the transition moment between the two configurations. This analysis leads to a simple and useful principle for *controlling the Q-band transition moment of porphyrin isomers and its derivatives:*
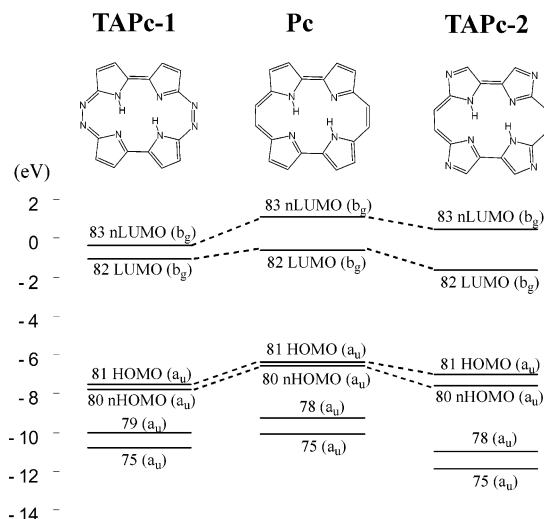

Figure 6. Hartree-Fock molecular orbital energy levels of **Pc** (center), **TAPc-1** (left), and **TAPc-2** (right). The dotted lines show the corresponding MOs among the three porphycenes.

tuning the energy gaps between the HOMO and next-HOMO and between the LUMO and next-LUMO. This can be a guiding principle for the practical design of pigments containing porphyrin isomers.

4. Controlling the Transition Moment of the Q-Band in Free-Base Porphycene

In the previous section, we discussed the excited states of **P**, **Pc**, **Cor**, and **hPc** and provided theoretical assignments for the experimental spectra. Based on this understanding of the excited states of porphyrin isomers, we attempted to design pigments with a stronger Q-band. Among the isomers, **Pc** has the most intense Q-band, and it was expected to be a suitable basic compound for pigment design. Here, we investigate the four porphycene derivatives namely two tetraza-substitutions (**TAPc**) and two dibenzo-substitutions (**exPc**) of **Pc**.

Tetraza-Substitution in Free-Base Porphycene. First, we briefly explain the tetraza-substitution effect observed in the free-base tetrazaporphyrin (**TAP**), in which four carbon atoms at meso-positions are substituted by nitrogen atoms. Since the next-HOMO of **P** has amplitude on the four N atoms as seen in Figure 4, N-substitution particularly stabilizes the next-HOMO levels and relaxes the near-degeneracy between the HOMO and next-HOMO levels. This strategy uses the fact that *the p-electron level of the nitrogen atoms is lower than that of the carbon atoms.* The resultant weight of the two configurations is approximately 2:1, and the intensity of the Q-band of **TAP** is approximately 100 times greater than that of **P** in the theoretical spectrum.[21a,d]

This tetraza-substitution is applied to the free-base **Pc**. First, the carbon atoms at 9-, 10-, 19-, and 20-positions of **Pc** are replaced by nitrogen atoms resulting in the compound, **TAPc-1** (Figure 1). This compound corresponds to an isomer of free-base tetrazaporphin. Considering the MO of **Pc** shown in Figure 4, this substitution would stabilize both the HOMO and next-HOMO levels, since these MOs have a similar amount of amplitude on the 9-, 10-, 19-, and 20-carbons. On the other hand, the stabilization of the next-LUMO level would be greater than that of LUMO, since next-LUMO has a relatively larger amplitude on the four carbons than LUMO. This preliminary consideration is confirmed by the orbital energy shown in Figure 6. The energy gap between LUMO and next-LUMO is much smaller than that in **Pc**, and this smaller gap would reduce the
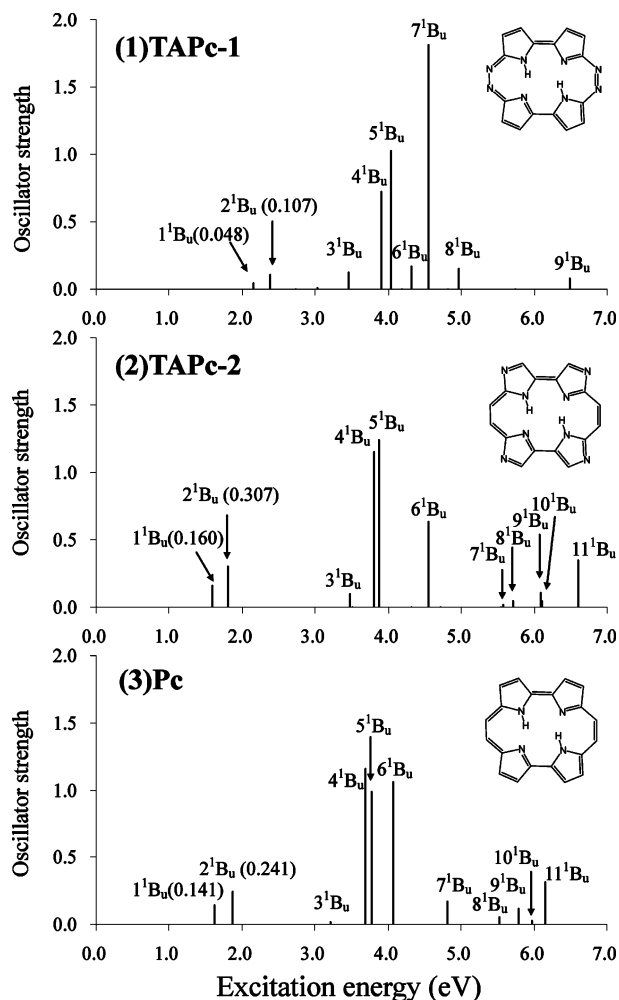
Figure 7. Excitation spectra of (1) **TAPc-1** and (2) **TAPc-2** calculated by the SAC-CI method. The excitation spectrum of (3) **Pc** is also shown for reference. Oscillator strength of the Q-band is shown in parentheses.

intensity of the Q-band of **TAPc-1**. As described in the previous section, the strong Q-band of **Pc** originates from the imbalanced weight of the two excited configurations. Therefore, if the LUMO and next-LUMO levels become closer, the weight of the two main configurations would become closer. This would enhance the cancellation of the transition moment between the two configurations in the **TAPc-1**.

Figure 7 compares the calculated excitation spectrum of **TAPc-1** and that of **Pc**. The oscillator strengths of the 1^1B_u and 2^1B_u states of **TAPc-1** are calculated to be 0.048 and 0.107 respectively, which are smaller than those of **Pc**. Table 6 shows the excited states of **TAPc-1**. As in **Pc**, the main configurations of the 1^1B_u and 2^1B_u states are composed of two excited configurations within the four orbitals. However, the weight of the two configurations is approximately 2:1, which is more balanced than that of **Pc** (4:1). This leads to a large cancellation of the transition moment of the Q-band of **TAPc-1**.

Other features found in the theoretical spectrum of **TAPc-1** are (1) the oscillator strength for the 3^1B_u state (X-band) is 10-fold greater than that of **Pc**, (2) the intensity of the 4^1B_u state (B-band) is relatively weak, and (3) the 7^1B_u state has a large oscillator strength. For the 3^1B_u state, the relative weight of the four-orbital excitation, 81 (HOMO) → 83 (next-LUMO), is larger than that of **Pc**, which contributes to the X-band intensity. For the 4^1B_u state, the main configuration is the excitation from the fifth orbital and the relative weight of the four-orbital excitation, 80 (next-HOMO) → 83 (next-LUMO), is small. On

the other hand, the 7^1B_u state (X′-band, a counterpart of the 4^1B_u state) has a major contribution by the excitation 80 → 83. Therefore, this configuration interaction transfers the transition intensity from B-band to X′-band.

The second tetrazaporphycene examined is 2,7,12,17-tetra-azaporphycene, **TAPc-2** (Figure 1 (f)). With this substitution, we tried to increase the energy-gap between HOMO (81) and next-HOMO (80) and that between LUMO (82) and next-LUMO (83). This design is based on the fact that LUMO and next-HOMO of **Pc** have a relatively larger amplitude on the 2-, 7-, 12-, and 17-th carbons compared to next-LUMO and HOMO, respectively.

As seen in Figure 6, LUMO and next-HOMO are stabilized more than next-LUMO and HOMO. The theoretical spectrum for **TAPc-2** is shown in Figure 7, and the excited states are summarized in Table 8. As expected from the orbital energy of the four-orbitals, the intensity of the Q-band (1^1B_u and 2^1B_u states) slightly increased to 0.160 and 0.307, respectively. As in **Pc**, the 1^1B_u state of **TAPc-2** is described by four-orbital excitations, 80(next-HOMO) → 82(LUMO) and 81(HOMO) → 83(next-LUMO). The ratio of the weight of these configurations is slightly more imbalanced than that of **Pc**. A similar result is obtained for the 2^1B_u state. The rest of the spectrum of **TAPc-2** is similar to that of **Pc**, except that new n-π^* transitions, 2^1A_u and 3^1A_u states, are calculated at 4.32 and 4.71 eV, respectively.

Ring-Extensions in Free-Base Porphycene. The second strategy is to extend the π-conjugation, i.e., to add an ethylene or *cis*-butadiene unit to the basic building block of **Pc**. A successful example of this strategy is the well-known pigment, phthalocyanine (PhCy). **PhCy** has four dibenzo-groups (*cis*-butadiene units) in four pyrrolic groups, in addition to tetra-aza substitution. *This strategy uses orbital interaction between the basic block and the substituents to control the orbital energy levels.* Since HOMO of **P** matches that of butadiene in terms of symmetry (see Figure 4), the interaction destabilizes HOMO of **PhCy**.[21e] The energy gap between HOMO and next-HOMO increases further, which enhances the Q-band intensity by 1000-fold larger than that of **P**. The ratio of the weight of the two configurations is approximately 6:1.[21e] This intensity enhancement originates not only from an imbalance in the weight but also from the transition moment of the configuration itself. However, the latter accounts for only a small portion of the increase in intensity.

We examined two ring-extended free-base porphycenes. The first is 3,6-,13,16-dibenzoporphycene, **exPc-1** (Figure 1 (g)), in which 3- and 6- carbons and 13- and 16- carbons are bridged by the ethylene units. This strategy is explained by a schematic diagram shown in Figure 8. There is a node at the C3−C6 and C13−C16 bonds in the LUMO of **Pc**, as is also observed in the LUMO of ethylene. Since these two LUMOs interact with each other, LUMO of **exPc-1** becomes lower than that of **Pc**. On the other hand, the next-LUMO of **Pc** and the LUMO of ethylene do not interact with each other due to the symmetry. Figure 9 shows that the LUMO level of **exPc-1** is slightly stabilized, and the energy gap between LUMO and next-LUMO becomes larger than that of **Pc**. Consequently, the HOMO−LUMO gap becomes smaller than that of **Pc**.

Figure 10 shows the theoretical spectrum of **exPc-1**. The spectrum is also compared to a recently reported experimental spectrum of 2,7,12,17-tetra-*tert*-butyl- 3,6-,13,16-dibenzopor-phycene.[18] Table 9 summarizes the excited states of **exPc-1** calculated by the SAC-CI method. First, we discuss the oscillator strength of the Q-bands. The 2^1B_u state (Q_2) has the 93→94 excitation as the main configuration, as shown in Table 9.

Porphyrin Isomers and Porphycene Derivatives

J. Phys. Chem. A, Vol. 109, No. 14, 2005 **3197**

TABLE 7: Excited States of TAPc-1 Calculated by the SAC-CI Method

		SAC-CI		
state	main configurations ($|C| > 0.25$)	nature	excitation energy (eV)	oscillator strength
$1^1B_u(Q_1)$	$0.64(80-82)-0.48(81-83)$	π-π^*	2.16	0.0479
$2^1B_u(Q_2)$	$0.68(81-82)+0.46(80-83)$	π-π^*	2.38	0.1067
1^1A_u	$0.94(74-82)$	n-π^*	2.72	0.0003
2^1A_u	$0.90(74-83)+0.30(73-84)$	n-π^*	3.04	5.4×10^{-3}
$3^1B_u(X)$	$0.81(79-82)-0.45(81-83)$	π-π^*	3.46	0.1226
$4^1B_u(B_1)$	$0.44(79-83)-0.43(80-83)$	π-π^*	3.91	0.7275
$5^1B_u(B_2)$	$-0.47(81-83)-0.46(80-82)+0.45(75-82)$	π-π^*	4.03	1.0258
	$-0.36(79-82)-0.26(80-83)$			
3^1A_u	$0.93(71-82)$	n-π^*	4.18	1.0×10^{-4}
$6^1B_u(Y)$	$-0.68(75-82)+0.56(79-83)$	π-π^*	4.32	0.1737
$7^1B_u(X')$	$-0.58(79-83)-0.58(80-83)+0.43(81-82)$	π-π^*	4.55	1.8168
4^1A_u	$-0.92(71-83)$	n-π^*	4.81	2.3×10^{-3}
$8^1B_u(Y')$	$0.92(75-83)$	π-π^*	4.96	0.1476
5^1A_u	$0.89(69-83)-0.28(68-84)$	n-π^*	5.75	2.0×10^{-4}
9^1B_u	$0.94(81-86)$	π-π^*	6.49	0.0807

TABLE 8: Excited States of TAPc-2 Calculated by the SAC-CI Method

		SAC-CI		
state	main configurations ($|C| > 0.25$)	nature	excitation energy (eV)	oscillator strength
$1^1B_u(Q_1)$	$0.80(80-82)-0.40(81-83)+0.29(81-82)$	π-π^*	1.59	0.1603
$2^1B_u(Q_2)$	$0.83(81-82)+0.32(80-83)-0.29(80-82)$	π-π^*	1.81	0.3074
$3^1B_u(X)$	$0.85(78-82)+0.35(81-83)$	π-π^*	3.48	0.0941
1^1A_u	$0.93(72-82)$	n-π^*	3.52	3.0×10^{-4}
$4^1B_u(B_1)$	$0.77(80-83)-0.35(81-82)-0.26(81-83)$	π-π^*	3.80	1.1539
	$+0.26(78-82)$			
$5^1B_u(B_2)$	$0.67(81-83)+0.39(80-83)+0.35(75-82)$	π-π^*	3.87	1.2448
	$+0.33(80-82)$			
2^1A_u	$0.94(70-82)$	n-π^*	4.32	0.0010
$6^1B_u(Y)$	$0.84(75-82)-0.26(81-83)$	π-π^*	4.55	0.6298
3^1A_u	$0.94(67-82)$	n-π^*	4.71	0.0000
4^1A_u	$0.91(72-83)$	n-π^*	5.54	6.0×10^{-4}
7^1B_u	$0.85(71-82)+0.26(81-86)+0.26(78-83)$	π-π^*	5.58	0.0201
$8^1B_u(X')$	$-0.83(78-83)+0.30(71-82)-0.26(81-86)$	π-π^*	5.71	0.0455
9^1B_u	$0.82(81-86)-0.30(78-83)-0.30(80-86)$	π-π^*	6.10	0.1100
10^1B_u	$-0.78(80-86)+0.43(75-83)-0.28(81-86)$	π-π^*	6.11	0.0491

Compared with the 2^1B_u state of **Pc**, the weight of the two main configurations is slightly more imbalanced in **exPc-1.** Therefore, the cancellation of the transition moment is more incomplete in **exPc-1**. In fact, the computed transition moments of the 2^1B_u states of **exPc-1** and **Pc** are 2.697 and 2.297 au, respectively, as shown in Table 11. However, the oscillator strength computed for **exPc-1** was smaller than that of **Pc**. This is due to the underestimation of the excitation energy in the calculation, since the oscillator strength is proportional to the excitation energy. Using the experimental excitation energy, the oscillator strength is computed to be larger than that of **Pc**.

Next, we briefly discuss other excited states of **exPc-1**. There are some important differences between the absorption spectra of **exPc-1** and **Pc**: (1) the assignment and appearance of the S_1-S_3 band, (2) the character of the 4^1B_u state, and (3) the character of the B-band. Regarding the first point, we noted that the S_1 and S_2 bands have Q-band character, even though the intensity of the S_3 band is relatively large. Actually, the S_3 band has the X-band character, and the previous semiempirical INDO/S calculation provided the same results.[18] With regard to the second point, the 4^1B_u state corresponds to the Y-band of **Pc**, i.e., the M-band of **P**. All of the $1^1B_u-4^1B_u$ states are excitations to LUMO, and the stabilization of LUMO causes a red-shift of these four states. In relation to the third point, the experimental absorption spectrum shows a broad B-band ranging from 3 to 4.5 eV. For S_4 (3.10 eV) and S_5 (3.35 eV), we assign the 5^1B_u and 6^1B_u states calculated at 3.22 and 3.36 eV, respectively. The 5^1B_u and 6^1B_u states have a large contribution

from non four-orbital excitations. The S_6 (3.66 eV) state is assigned to the 7^1B_u (4.04 eV) state. The 7^1B_u state has the same character as the 7^1B_u state (X'-band) of **Pc**.

We noted several significant differences between the SAC-CI and CNDO/S results as seen in Table 9. First, the order of the excited states is reversed between the 1^1B_u and 2^1B_u states and between the 5^1B_u and 6^1B_u states. Second, the INDO result lacks the 4^1B_u state. Third, there are few corresponding features in the character of the excited states higher than the 6^1B_u states.

The second substituted porphycene, 9,10-,19,20-dibenzopor-phycene (**exPc-2**, Figure 1 (h)), has two butadiene units that bridge the 9- and 10-carbons and 19- and 20-carbons. Figure 4 shows that LUMO of **Pc** does not have a node at C9−C10 and C19−C20 bonds, while HOMO has a node at these two bonds. Considering the symmetry of MOs, LUMO and HOMO of **Pc** interact with the butadiene MOs as schematically shown in Figure 8. Figure 9 confirms that HOMO of **exPc-2** shifted significantly to a higher energy region, whereas LUMO moved to a lower energy region.

The SAC-CI theoretical spectrum of **exPc-2** is shown in Figure 10, and the details of the excited states are summarized in Table 10. The 1^1B_u state calculated at 0.77 eV is HOMO−LUMO excitation. As seen in Table 10, the transition moment of the 1^1B_u state is 2.812 au, which is much larger than that of the 2^1B_u state of **Pc** (2.297 au). However, the calculated oscillator strength is 0.149 au, which is smaller than that of the 2^1B_u state of **Pc**. This is again due to the spectral red shift caused by the small HOMO−LUMO gap, which reduces the calculated
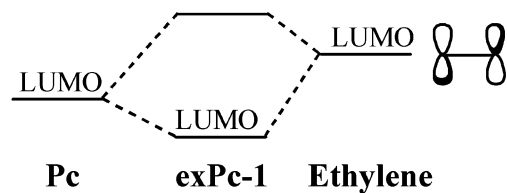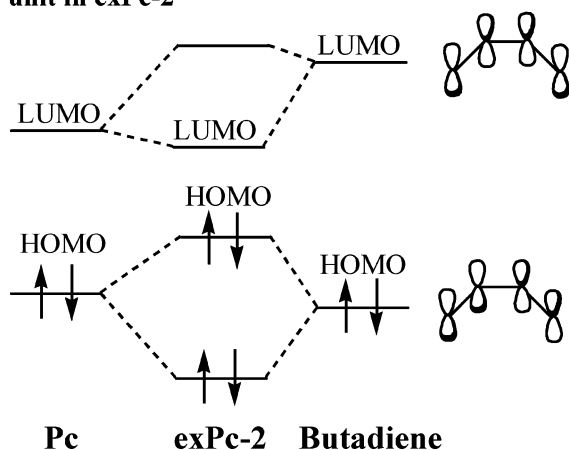
(1)Interaction between Pc and ethylene unit in exPc-1

(2)Interaction between Pc and butadiene unit in exPc-2

Figure 8. Schematic diagrams showing (1) the interaction between **Pc** and the ethylene unit in **exPc-1** and (2) the interaction between **Pc** and the butadiene unit in **exPc-2**.
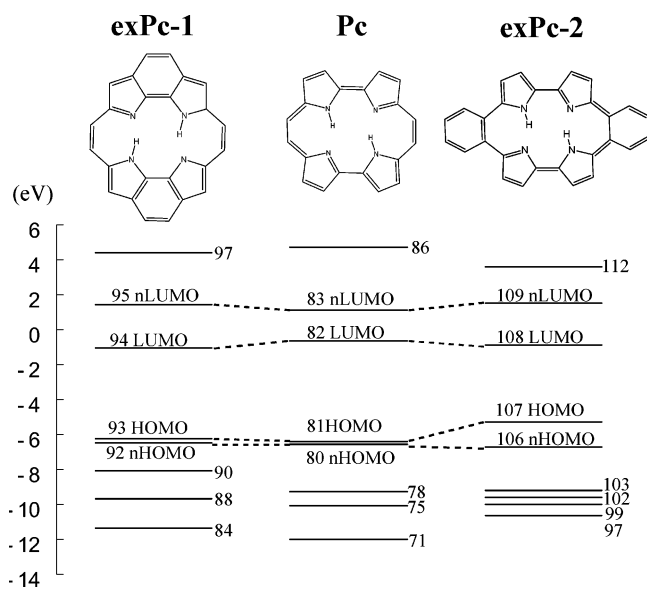

Figure 9. Hartree-Fock molecular orbital energy levels of **Pc** (center), **exPc-1** (left), and **exPc-2** (right). The dotted lines show the corresponding MOs among the three porphycenes.

oscillator strength. The following points should be noted (1) the X-band, 3^1B_u state, is much less intense than that of **exPc-1**, (2) the 4^1B_u and 6^1B_u states are characterized as B-bands, and (3) the 5^1B_u state corresponds to the Y-band of **Pc**, even though the oscillator strength is rather strong.

5. Conclusion

The excited states of free-base porphyrin isomers, porphin (**P**), porphycene (**Pc**), corrphycene (**Cor**), and hemiporphycene
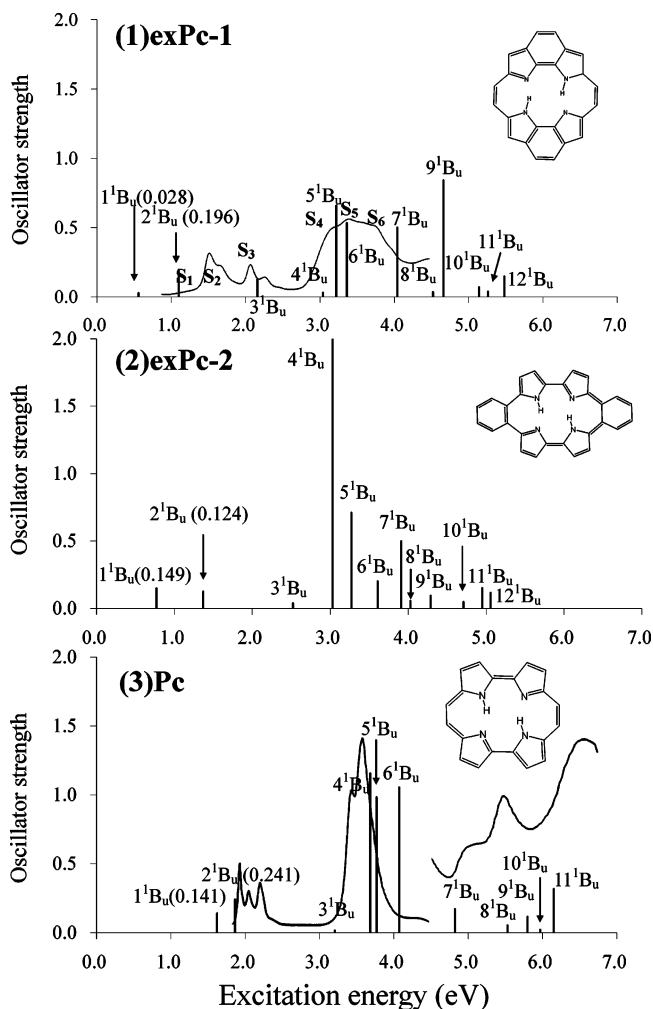

Figure 10. Excitation spectra of (1) **exPc-1** and (2) **exPc-2** calculated by the SAC-CI method. The excitation spectrum of (3) **Pc** is also shown for reference. The oscillator strength of the Q-band is shown in parentheses. For **exPc-1** and **Pc**, the theoretical spectra are compared with the experimental spectra. For **exPc-1**, tetra-*tert*-butyldibenzopor-phycene[18] is used. The oscillator strength of the experiments is shown in arbitrary units.

(**hPc**), were studied by the SAC-CI method. This is the first attempt to provide theoretical assignments to the absorption spectra of these porphyrin isomers using a state-of-the-art correlation method. The present results agree reasonably with the trend of the experiments. The average error in the excitation energy was 0.17 eV for the four compounds. For **Pc**, we examined the basis sets effects since the error was relatively large. The results showed a uniform shift of about 0.2−0.3 eV as shown in Table 4, which does not affect the assignment given by the DZ(d,p) level calculations. We also investigated the solvation effect, and its result was similar to that obtained by the gas-phase calculation. An exception was that the X-band shifted to a higher energy region, since the X-band has a partial charge-transfer character.

The spectral features of the isomers reflect the Hartree−Fock orbital energies for the four-orbitals. A large energy gap between LUMO and next-LUMO causes the imbalanced weight of the two main configurations of the Q-band. Thus, **Pc** has the highest Q-band intensity among these four compounds. The low-lying LUMO of **Pc** also results in the X-band that appears on the lower energy side of the B-band.

As reported in the previous studies,[21a,b,22] the B-band of **P** is described by the "five-orbital model". The fifth orbital also

Porphyrin Isomers and Porphycene Derivatives

J. Phys. Chem. A, Vol. 109, No. 14, 2005 **3199**

TABLE 9: Excited States of ExPc-1 Calculated by the SAC-CI Method

state	main configurations ($|C| > 0.25$)	nature	SAC-CI excitation energy (eV)	SAC-CI oscillator strength	INDO/S[a] excitation energy (eV)	INDO/S[a] oscillator strength	exptl[b] excitation energy (eV)
$1^1B_u(Q_1)$	$0.84(92-94)-0.34(90-94)$	π-π*	0.56	0.0275	1.79	0.30	$1.30(S_1)$
$2^1B_u(Q_2)$	$-0.87(93-94)+0.26(92-95)$	π-π*	1.10	0.1958	1.43	0.11	$1.48(S_2)$
3^1B_u	$0.81(90-94)+0.37(93-95)$ $+0.27(92-94)$	π-π*	2.16	0.1296	2.35	0.06	$2.11(S_3)$
4^1B_u	$0.72(88-94)-0.55(92-95)$	π-π*	3.04	0.0302			
$5^1B_u(B_1)$	$0.61(92-95)+0.53(88-94)$ $-0.32(90-95)+0.29(93-94)$	π-π*	3.22	0.6581	3.39	0.95	$3.10(S_4)$
$6^1B_u(B_2)$	$-0.76(93-95)-0.26(91-96)$	π-π*	3.36	0.5331	3.23	1.16	$3.35(S_5)$
7^1B_u	$0.84(90-95)+0.34(92-95)$	π-π*	4.04	0.4998			$3.66(S_6)$
8^1B_u	$0.87(84-94)$	π-π*	4.52	0.0362			
9^1B_u	$0.84(91-96)$	π-π*	4.66	0.8410			
10^1B_u	$0.88(88-95)$	π-π*	5.14	0.0697			
11^1B_u	$0.91(93-97)$	π-π*	5.26	0.0380			
12^1B_u	$0.87(92-97)$	π-π*	5.48	1.4062			

[a] Reference 18. [b] Excitation energy read from spectral chart in ref 18.

TABLE 10: Excited States of ExPc-2 Calculated by the SAC-CI Method

state	main configurations ($|C| > 0.25$)	nature	SAC-CI excitation energy (eV)	SAC-CI oscillator strength
$1^1B_u(Q_1)$	$0.90(107-108)$	π-π*	0.77	0.1485
$2^1B_u(Q_2)$	$-0.77(106-108)-0.47(107-109)$	π-π*	1.37	0.1244
3^1B_u	$0.89(103-108)$	π-π*	2.52	0.0376
$4^1B_u(B_1)$	$-0.72(107-109)+0.40(106-108)$ $-0.39(99-108)$	π-π*	3.03	2.0031
5^1B_u	$-0.79(99-108)-0.28(106-108)$ $+0.27(107-109)$	π-π*	3.27	0.7100
$6^1B_u(B_2)$	$-0.70(106-109)-0.55(102-108)$	π-π*	3.61	0.2013
7^1B_u	$0.61(102-108)-0.58(106-109)$ $+0.30(107-112)$	π-π*	3.91	0.4989
8^1B_u	$0.85(107-112)-0.35(102-108)$	π-π*	4.03	0.0560
9^1B_u	$-0.80(97-108)+0.28(107-114)$ $+0.27(107-108,105-108)$	π-π*	4.29	0.0929
10^1B_u	$0.80(103-109)+0.25(107-114)$	π-π*	4.71	0.0483
11^1B_u	$-0.78(106-112)+0.33(102-109)$	π-π*	4.95	0.1507
12^1B_u	$+0.81(107-114)-0.32(103-109)$ $+0.26(97-108)-0.28(107-113,107-108)$	π-π*	5.06	0.1159

TABLE 11: Transition Moment, Excitation Energy, and Oscillator Strength of Q-bands for Pc, TAPc-1, TAPc-2, ExPc-1, and ExPc-2

	Pc Q_1	Pc Q_2	TAPc-1 Q_1	TAPc-1 Q_2	TAPc-2 Q_1	TAPc-2 Q_2	exPc-1 Q_1	exPc-1 Q_2	exPc-2 Q_1	exPc-2 Q_2
TM[a]	1.884	2.297	0.953	1.352	2.027	2.635	1.415	2.697	2.812	1.922
EE[b](calc.)	1.62	1.86	2.16	2.38	1.59	1.81	0.56	1.10	0.77	1.37
EE(exptl.)	1.96	2.07					1.30	1.48		
OS(calc.)[c]	0.141	0.241	0.048	0.107	0.160	0.307	0.028	0.196	0.149	0.124
OS(scaled)[d]	0.228	0.256					0.065	0.264		

[a] Transition moment (au). [b] Excitation energy (eV). [c] Oscillator strength. [d] Oscillator strength using the experimental excitation energy.

contributes to the B-bands of all the porphyrin isomers in this study. The B-bands of **Cor** and **hPc** are characterized as a mixture of the 2^1B_{3u} (B-band) and the optically forbidden 1^1B_{1g} states of **P**. This is due to the symmetry lowering in the molecular structure. Consequently, the main configurations of the B-band are described by six orbitals (in the "six-orbital" model). This information is useful for pigment design.

Based on the present and previous studies,[21d,e,l] we attempted to control the Q-band transition moment of **Pc** by modifying the four-orbital model. We proposed two kinds of tetra-aza substitutions, **TAPc-1** and **TAPc-2**, and two kinds of ring-extension (dibenzo substitutions), **exPc-1** and **exPc-2**. **TAPc-2** has a LUMO-next-LUMO gap larger than that of **Pc**. Accordingly, the theoretical spectrum of **TAPc-2** shows a greater Q-band intensity. For **exPc-1** and **exPc-2**, the transition moments

of the excited states were much larger than those of **Pc** as shown in Table 11. However, the oscillator strength was calculated to be slightly smaller than that of **Pc**, since the calculated excitation energy of the Q-band is much smaller than expected. Thus, to increase the intensity of the Q-band the effect of the excitation energy has to be considered.

Although the four-orbital model is a qualitative model, it can be quantitatively applied to the Q-band. Therefore, modification to the four-orbital model would provide a simple and promising strategy which can serve as a guiding principle for designing the excited states of the Q-band.

References and Notes

(1) Bettersby, A. R.; Fookes, C. J. R.; Matcham, G. W. J.; McDonald, E. *Nature (London)* **1980**, *285*, 17.

(2) Porphyrin Photosensitization. *Advances in Experimental Medicine and Biology 160*; Kessel, D., Dougherty, T., Eds.; Plenum: New York, 1983.

(3) *Porphyrins in Tumor Phototherapy*; Andreoni, A., Cubeddo, R., Eds.; Plenum: New York, 1984.

(4) Vogel, E.; Köcher, M.; Schmickler, H.; Lex, J. *Angew. Chem.* **1986**, *98*, 262; *Angew. Chem., Int. Ed. Engl.* **1986**, *25*, 257.

(5) Waluk, J.; Müller, M.; Swiderek, P.; Köcher, M.; Vogel, E.; Hohlneicher, G.; Michl, J. *J. Am. Chem. Soc.* **1991**, *113*, 5511.

(6) Waluk, J.; Michl, J. *J. Org. Chem.* **1991**, *56*, 2729.

(7) Sessler, J. L.; Brucker, E. A.; Weghorn, S. J.; Kisters, M.; Schäfer, M.; Lax, J.; Vogel, E. *Angew. Chem.* **1994**, *106*, 2402; *Angew. Chem., Int. Ed. Engl.* **1994**, *33*, 2308.

(8) Aukauloo, M. A.; Guilard, R. *New J. Chem.* **1994**, *18*, 1205.

(9) Callot, H. J.; Rohrer, A.; Tschamber, T.; Mets, B. *New J. Chem.* **1995**, *19*, 155.

(10) Vogel, E.; Bröring, M.; Weghorn, S. J.; Schloz, P.; Deponte, R.; Lex, J.; Schmickler, H.; Schaffner, K.; Braslarsky, S. E.; Müller, M.; Pörting, S.; Fowler, C. J.; Sessler, J. L. *Angew. Chem., Int. Ed. Engl.* **1997**, *36*, 1651; *Angew. Chem.* **1997**, *109*, 1725.

(11) Aramendia, P. F.; Redmond. R. W.; Nonell, S.; Schuster, W.; Braslavsky S. E.; Schaffner, K.; Vogel, E. *Photochem. Photobiol.* **1986**, *44*, 555.

(12) Braslavsky S. E.; Müller, M.; Mátire, D. O.; Pörting, S.; Bertolotti, S. G.; Chakravoti, S.; Koç-Weier, G.; Knipp, B.; Schaffner, K. *J. Photochem. Photobiol. B* **1997**, *40*, 191.

(13) Wu, Y.-D.; Chan, K. W. K.; Yip, C.-P.; Vogel, E.; Plattner, D. A.; Houk, K. N. *J. Org. Chem.* **1997**, *62*, 9240−9250.

(14) Kozlowski, P. M.; Zgierski, M. Z.; Baker, J. *J. Chem. Phys.* **1998**, *109*, 5905−5913.

(15) Malsch, K.; Roeb, M.; Karuth, V.; Hohlneiher, G. *Chem. Phys.* **1998**, *227*, 331−348.

(16) Kay, C. W. M.; Gromadecki, U.; Törring, J. T.; Weber, S. *Mol. Phys.* **2001**, *99*, 1413−1420.

(17) Vogel, E.; Bröring, M.; Fink, J.; Rosen, D.; Schmickler, H.; Lex, J.; Chan, K. W. K.; Wu, T.-D.; Plattner, S. A.; Nendel, M.; Houk, K. N. *Angew. Chem., Int. Ed. Engl.* **1995**, *34*, 2511−2514.

(18) Dobcowski, J.; Galievsky, V.; Starukhin, A.; Vogel, E.; Waluk, J. *J. Phys. Chem. A* **1998**, *102*, 4966−4971.

(19) Vogel, E. *J. Heterocycl. Chem.* **1996**, *33*, 1461.

(20) Gouterman, M. *J. Mol. Spectrosc.* **1961**, *6*, 138.

(21) Free-base porphin: (a) Nakatsuji, H.; Hasegawa, J.; Hada, M. *J. Chem. Phys.* **1996**, *104*, 2321. (b) Tokita, Y.; Hasegawa, J.; Nakatsuji, H. *J. Phys. Chem.* **1998**, *102*, 1834−1849. Mg-porphin: (c) Hasegawa, J.; Hada, M.; Nonoguchi, M.; Nakatsuji, H. *Chem. Phys. Lett.* **1996**, *250*, 159. Free-base tetrazaporphin: (d) Toyota, K.; Hasegawa, J.; Nakatsuji, H. *Chem. Phys. Lett.* **1996**, *250*, 437. (e) Free-base phthalocyanine: Toyota, K.; Hasegawa, J.; Nakatsuji, H. *J. Phys. Chem.* **1997**, *101*, 446−451. Oxy-heme: (f) Nakatsuji, H.; Hasegawa, J.; Ueda, H.; Hada, M. *Chem. Phys. Lett.* **1996**, *250*, 379. Carboxyheme: (g) Nakatsuji, H.; Tokita, Y.; Hasegawa, J.; Hada, M. *Chem. Phys. Lett.* **1996**, *256*, 220−228. Hemoglobin CO and Horseradish Peroxidase CO: (h) Tokita, Y.; Nakatsuji, H. *J. Phys. Chem. B* **1997**, *101*, 3281−3289. Special pair: (i) Hasegawa, J.; Ohkawa, K.; Nakatsuji, H. *J. Phys. Chem.* **1998**, *102*, 10410. P450−CO: (j) Miyahara, T.; Tokita, Y.; Nakatsuji H. *J. Phys. Chem. B* **2001**, *105*, 7341−7352. Four hemes (c-552, 554, 556, and 559) in the reaction center of *Rhodopseudomonas viridis*: (k) Ohkawa, K.; Hada, M.; Nakatsuji, H. *J. Porphyrins Phthalocyanines* **2001**, *5*, 256−266. (l) Hasegawa, J.; Ozeki, Y.; Ohkawa, K.; Hada, M.; Nakatsuji, H. *J. Phys. Chem. B* **1998**, *102*, 1320−1326.

(22) Petke, J. D.; Maggiora, G. M.; Shipman, L. L. Christofferson, R. *J. Mol. Spectrosc.* **1987**, *71*, 64−84.

(23) Nakatsuji, H.; Hirao, K. *J. Chem. Phys.* **1978**, *68*, 2053.

(24) Nakatsuji, H. *Chem. Phys. Lett.* **1978**, *59*, 362; **1989**, *67*, 329; **1989**, *67*, 334.

(25) Nakatsuji, H. In *Computational Chemistry, Reviews of Current Trends*; Leszczynski, J., Ed.; World Scientific: Singapore, 1996; Vol. 2, pp 62−124.

(26) Linstead, R. P.; Whalley, M. *J. Chem Soc.* **1952**, *4839*.

(27) Thomas, A. L. *Phthalocyanine Research and Applications*; CRC Press: 1990.

(28) (a) Hohenberg, P.; Kohn. W. *Phys. Rev.* **1964**, *136*, B864. (b) Kohn, W.; Sham, L. J. *Phys. Rev.* **1965**, A1133. (c) *The Challenge of d and f Electrons*; Salahub, D. R., Zerner, M. C., Eds.; ACS: Washington, DC, 1989. (d) Parr, R. G.; Yang, W. *Density-functional Theory of Atoms and Molecules*; Oxford University Press: Oxford, 1989.

(29) (a) Lee, C.; Yang, W.; Parr, R. G. *Phys. Rev.* **1988**, *37*, 785. (b) Becke, A. D. *J. Chem. Phys.* **1993**, *98*, 5648.

(30) Wu, Y.-D.; Chan, K. W. K. *J. Mol. Struct. (THEOCHEM)* **1997**, *398−399*, 325−332.

(31) Huzinaga, S.; Andzelm, J.; Krovkowski, M.; Radzio-Andzelm, E.; Sakai, Y.; Tatewaki, H. *Gaussian basis set for molecular calculation*; Elsevier: New York, 1984.

(32) Huzinaga, S. *J. Chem. Phys.* **1965**, *42*, 1293.

(33) Hehre, W. J.; Ditchfield, R.; Pople, J. A. *J. Chem. Phys.* **1972**, *56*, 2257.

(34) Hariharan, P. C.; Pople, J. A. *Theor. Chim. Acta* **1973**, *28*, 213.

(35) Nakatsuji, H. *Chem. Phys.* **1983**, *75*, 425.

(36) Dunning, T. H., Jr. *J. Chem. Phys.* **1971**, *55*, 716.

(37) Cancés, M. T.; Mennucci, B.; Tomasi, J. *J. Chem. Phys.* **1997**, *107*, 3210.

(38) Frisch, M. J.; Trucks, G. W.; Schlegel, H. B.; Scuseria, G. E.; Robb, M. A.; Cheeseman, J. R.; Montgomery, J. A., Jr.; Vreven, T.; Kudin, K. N.; Burant, J. C.; Millam, J. M.; Iyengar, S. S.; Tomasi, J.; Barone, V.; Mennucci, B.; Cossi, M.; Scalmani, G.; Rega, N.; Petersson, G. A.; Nakatsuji, H.; Hada, M.; Ehara, M.; Toyota, K.; Fukuda, R.; Hasegawa, J.; Ishida, M.; Nakajima, T.; Honda, Y.; Kitao, O.; Nakai, H.; Klene, M.; Li, X.; Knox, J. E.; Hratchian, H. P.; Cross, J. B.; Adamo, C.; Jaramillo, J.; Gomperts, R.; Stratmann, R. E.; Yazyev, O.; Austin, A. J.; Cammi, R.; Pomelli, C.; Ochterski, J. W.; Ayala, P. Y.; Morokuma, K.; Voth, G. A.; Salvador; Dannenberg, J. J.; Zakrzewski, V. G.; Dapprich, S.; Daniels, A. D.; Strain, M. C.; Farkas, O.; Malick, D. K.; Rabuck, A. D.; Raghavachari, K.; Foresman, J. B.; Ortiz, J. V.; Cui, Q.; Baboul, A. G.; Clifford, S.; Cioslowski, J.; Stefanov, B. B.; Liu, G.; Liashenko, A.; Piskorz, P.; Komaromi, I.; Martin, R. L.; Fox, D. J.; Keith, T.; Al-Laham, M. A.; Peng, C. Y.; Nanayakkara, A.; Challacombe, M.; Gill, P. M. W.; Johnson, B.; Chen, W.; Wong, M. W.; Gonzalez, C.; Pople, J. A. *Gaussian 03*, revision B.01; Gaussian, Inc.: Pittsburgh, PA, 2003.

(39) Schaftenaar, G.; Noordik, J. H. Molden: a pre- and postprocessing program for molecular and electronic structures. *J. Comput.-Aided Mol. Des.* **2000**, *14*, 123−134.

(40) Free-base porphin: (a) Nagashima, U.; Takada, T.; Ohno, K. *J. Chem. Phys.* **1986**, *85*, 4524. (b) Yamamoto, Y.; Noro, T.; Ohno, K. *Int. J. Quantum Chem.* **1992**, *42*, 1563.

(41) Free-base porphin: (a) Serrano-Andrés, L.; Merchán, M.; Rubio, M.; Roos, B. O. *Chem. Phys. Lett.* **1998**, *295*, 195−203. (b) Merchán, M.; Ortí, E.; Roos, B. O. *Chem. Phys. Lett.* **1994**, *226*, 27. Mg-porphin: Rubio, M.; Roos, B. O.; Serrano-Andrés, L.; Merchán, M. *J. Chem. Phys.* **1999**, *110*, 7202−7209.

(42) Free-base porphin: (a) Nooijen, M.; Bartlett, R. J. *J. Chem. Phys.* **1997**, *106*, 6449. (b) Gwaltney, S. R.; Bartlett, R. J. *J. Chem. Phys.* **1998**, *108*, 6790.

(43) Edwards, L.; Dolphin, D. H.; Gouterman, M.; Adler, A. D. *J. Mol. Spectrosc.* **1971**, *38*, 16.

(44) Zandler, M. E.; D'Souza, F. *J. Mol. Struct. (THEOCHEM)* **1997**, *401*, 301−314.